NASA/CR-20240012465



Secondary Electron Suppression With Carbonized Aerogels

JR Dennsion
Utah State University, Logan, Utah

October 2024

NASA STI Program . . . in Profile

Since its founding, NASA has been dedicated to the advancement of aeronautics and space science. The NASA scientific and technical information (STI) program plays a key part in helping NASA maintain this important role.

The NASA STI program operates under the auspices of the Agency Chief Information Officer. It collects, organizes, provides for archiving, and disseminates NASA's STI. The NASA STI program provides access to the NTRS Registered and its public interface, the NASA Technical Reports Server, thus providing one of the largest collections of aeronautical and space science STI in the world. Results are published in both non-NASA channels and by NASA in the NASA STI Report Series, which includes the following report types:

- TECHNICAL PUBLICATION.
  Reports of completed research or a major significant phase of research that present the results of NASA programs and include extensive data or theoretical analysis. Includes compilations of significant scientific and technical data and information deemed to be of continuing reference value. NASA counterpart of peer-reviewed formal professional papers but has less stringent limitations on manuscript length and extent of graphic presentations.

- TECHNICAL MEMORANDUM.
  Scientific and technical findings that are preliminary or of specialized interest, e.g., quick release reports, working papers, and bibliographies that contain minimal annotation. Does not contain extensive analysis.

- CONTRACTOR REPORT.
  Scientific and technical findings by NASA-sponsored contractors and grantees.

- CONFERENCE PUBLICATION.
  Collected papers from scientific and technical conferences, symposia, seminars, or other meetings sponsored or cosponsored by NASA.

- SPECIAL PUBLICATION.
  Scientific, technical, or historical information from NASA programs, projects, and missions, often concerned with subjects having substantial public interest.

- TECHNICAL TRANSLATION.
  English-language translations of foreign scientific and technical material pertinent to NASA's mission.

Specialized services also include organizing and publishing research results, distributing specialized research announcements and feeds, providing information desk and personal search support, and enabling data exchange services.

For more information about the NASA STI program, see the following:

- Access the NASA STI program home page at http://www.sti.nasa.gov

NASA/CR-20240012465



Secondary Electron Suppression With Carbonized Aerogels

JR Dennsion
Utah State University, Logan, Utah

National Aeronautics and
Space Administration

Glenn Research Center
Cleveland, Ohio 44135

October 2024

Trade names and trademarks are used in this report for identification only. Their usage does not constitute an official endorsement, either expressed or implied, by the National Aeronautics and Space Administration.

Level of Review: This material has been technically reviewed by NASA expert reviewer(s).

This report is available in electronic form at https://www.sti.nasa.gov/ and https://ntrs.nasa.gov/

NASA STI Program/Mail Stop 050
NASA Langley Research Center
Hampton, VA 23681-2199

Secondary Electron Suppression with Carbonized Aerogels

Report

JR Dennison
Utah State University
Logan, Utah 84322



Contact Information

NASA Glenn Research Center.
21000 Brookpark Rd.
Cleveland, OH 44135-3127

Utah State University Materials Physics Group
JR Dennison
Professor, Physics Department

4415 Old Main Hill
Logan, UT 84322 USA
telephone +1 435 797 2936
Cell +1 435 232 6743
fax +1 435 797 2946
JR.Dennison@usu.edu

UTAH STATE UNIVERSITY FINANCIAL POINT OF CONTACT
Devin Hansen
Contract & Grant Officer, Sponsored Programs,
Office of Research and Graduate Studies, Utah State University, Logan, UT
84322 Office: (435) 797-9153
Devin.Hansen@usu.edu

USU Materials Physics Group

(Back row Left to Right) Ben Russon, Heather Zollinger, Zack Gibson, Matthew Robertson, Jordan Lee, David King

(Front row Left to Right) Justin Christensen, Alexandra Nelson, Alex Souvall, Greg Wilson, Allen Andersen, JR Dennison, Windy Olsen

(Not pictured) Brian Wood, Vladimir Zavyalov, Jodie Gillespie, Ashlan Keller, Tanner Linton, Jonh Mojica Decena, Tyler Kippen



USU MPG Webpage

http://digitalcommons.usu.edu/mp/

Report Outline

Project Overview
- Overview of proposed work
- Tests Completed
- Summary of Results

Sample Preparation and Characterization
- Sample Photos
- Electron Range
- Sample Preparation
- SEM/EDX Measurements
- Optical Reflectivity Measurements

Electron Emission Test Results
- Instrumentation
- Yield Models
- Electron Yield and Emission Spectra Measurements
- Comparison with Previous Studies and Standards

References

NASA/GRC

Secondary Electron Suppression with Carbonized Aerogels

Intermediate Report

Project Overview

Overview of proposed work
Tests Completed
Summary of Results

Project Overview

PROJECT GOAL

The goal addressed by this project is reduced DC power for high data rate RF communications by increasing the efficiency of traveling Wave Tubes (TWT) for RF communication, which are used by most space missions for communication and radio science at microwave frequencies. The capability needed is a robust electron collector surface with a secondary electron emission lower than ordinary graphite, which is the state of the art. While it is known that replacing a smooth surface with a textured one will reduce secondary electron emission, no robust textured surface is known.

Carbonized polyimide aerogels promise the necessary robustness along with reduced secondary electron emission, allowing further improvement of TWT efficiency, achieving a very good return on the low investment made. Aerogels are known to be robust materials, and carbon aerogels are expected to have low secondary electron emission because of their open surface structure. The objective of this proposal is to demonstrate the low secondary electron emission of carbon aerogels and their robustness.

TASK DESCRIPTION:

The objective of the measurements conducted as part of this study is to provide measurements of electron emission of specific coating materials. The Utah State University (USU) Materials Physics Group (MPG) will performed the measurement of total, backscattered, and secondary electron yield and electron emission spectra for the carbon spacecraft materials.

For **Phase I** measurements he MPG will measure the total, secondary, and backscatter yields of approximately *four* conductive carbon aerogel materials, with thicknesses well in excess of the range of 30 keV electron used for emission tests. Measurements will be made in the MPG Electron Emission Test Chamber, at a base pressure vacuum <10^{-8} Torr. State-of-the-art pulsed-yield methods developed at USU for measuring the yields of highly charged samples using their Hemispherical Grid Retarding Field Analyzer will be used. Typical ~10 nA/cm^2, ~5 µs, ~0.5 nJ pulses will minimize any sample heating of the thin filament aerogels. Yield measurements will be made at approximately 30 energies from ~20 eV to ~30 keV at room temperature. The first and second crossover energies, maximum yields, and energies of maximum yields will be determined. Measurements will be made of the electron emission spectra. Standard analysis and error analysis of the yields will be made, including parameterized fits (including NASCAP fits) to the total, secondary, and backscatter yield curves and the emission spectra.

The two materials deemed most promising will be evaluated at two additional thicknesses, a thin sample with thickness less than the range of incident electrons at the energy of maximum total yield and an intermediate thickness. These two promising materials will also be subjected to a typical launch vibration profile on a shaker table and subsequently re-evaluated to determine if there are any effects from intense vibration.

A subsequent set of measurements is proposed for **Phase II** follow up studies to evaluate the effects of aerogel heating on electron emission. Pulsed electron yields and emission spectra of the two promising materials will be tested at elevated temperatures of ~400 K and ~500 K. Electron yields and emission spectra of samples of these materials will also be made using continuous current methods at ~1 nA/cm^2, ~10 nA/cm^2, ~100 nA/cm^2; current densities will be chosen to produce significant Joule heating of the aerogel surface which will have reduced thermal conductivity due to the filament nature of the samples. Sample and substrate temperatures will be monitored by both thermocouples and non-contact IR thermometry.

Secondary Electron Suppression with Carbonized Aerogels

GRC Lead/PI: Dale Force

Project Vision/Description
- To use carbon aerogels to increase the efficiency of traveling wave tubes (TWT) for space missions.

Project Goal
- To demonstrate that carbon aerogels are a robust materials to reduce secondary electron emission energy losses

Project Objective
- Measure secondary electron emission from carbon aerogels

Strategic Alignment
- SMD, HEOMD, TA 5.2.2, High Data Rate Communications
- High Data Rate Communications, TA 5.2.2
- Communications Technology & Development, Lead Center TWT

Technology Readiness Goal
Starting TRL: [2]
Target/Ending TRL: [5]

Key Technical Challenge(s)
- Obtain a variety of aerogel samples for measurement
- Make secondary electron emission measurements
- Determine best aerogel for electron collector use

Infusion Strategy/Plan
- Work with L-3 TWT groups to demonstrate use of aerogels in TWTs to reduce secondary electron emission and increase efficiency. L-3 is the sole US manufacturer of space TWTs

Anticipated Benefits
- Reduced power use in space TWTs for NASA, DOD, and commercial missions
- Reduced power use in electron beam devices in all environments



Carbon Aerogel Block

Project Approach/Plan
- Obtain carbon aerogel samples with varying parameters
- Measure secondary electron emission from aerogel samples

Key Milestones and Dates
- Aerogel samples ordered November 2016
- First secondary electron measurements February 2017
- Secondary electron measurements complete May 2017
- Final Report September 2017

NASA Team Member(s)
- Dale Force/LCF
- Marie Piasecki/LCF
- Dr. Maryann Meador/LMN

External Partner
- Dr. J. R. Dennison/Utah State University

ROM Estimate - Civil Servant Hours: 0.4 FTE

ROM Estimate - Procurement Cost ($K): 50

Tests Completed

- Electron Yield Measurements
  - Low energy (15-5000 eV)
  - High energy (7.5-30 keV)
- Electron Emission Energy Spectra
  - Measured emitted kinetic energies of 0-60 eV
- Samples Tested
  - CRF Aerogel
  - POCO Foam
  - Glassy Carbon
  - Graphite
  - Carbon Fiber
  - Carbonized Polyimide
  - HOPG (USU Sample from Union Carbide)

Sample	Sample Prep.	In Chamber	Low Energy Yields (20 eV to 5 keV)			High Energy Yields (5 keV to 30 keV)			Emission Spectra	Characterization			
			TEY	SEY	BSEY	TEY	SEY	BSEY		Optical Photos	SEM	EDX	Reflect-ivity
Glassy Carbon	X	X	X	X	X	X	X	X	X	X			
Ordinary Carbon	X	X	X	X	X	X	X	X	X	X			
Carbon Fiber	X	X	X	X	X	X	X	X	X	X			
Carbonized PI	X	X	X	X	X	X	X	X	X	X			
CRF Aerogel	X	X	X	X	X	X	X	X	X	X			
Poco Foam	X	X	X	X	X	X	X	X	X	X			
HPOG Graphite	X	X	X	X	X	X	X	X	X	X			X
Material 1 Shake Test													
Material 2 Shake Test													
Material 1 High Temperature Test													
Material 2 High Temperature Test													

Conclusion Based on Measured Yields

Overall Results

- Samples all have similar TEY, BSEY and SEY
- All carbon samples have same low E_{max} of ~250-350 eV. These are somewhat higher than the HOPG E_{max} of ~190 eV.
- Poco Foam has the best overall low TEY σ_{max} performance

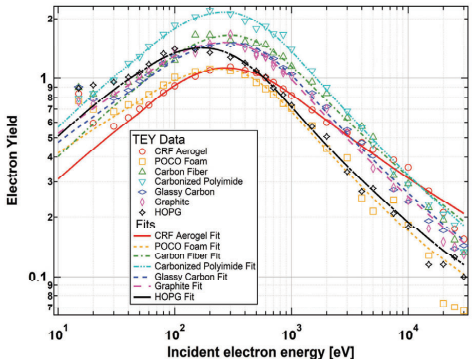
SEY Yields

- Poco Foam and CRF Aerogel have the best overall SEY δ_{max} performance
- Poco Foam and HOPG have the lowest SEY δ_{max} >1000 eV
- CRF Aerogel and HOPG have the lowest SEY δ_{max} <400 eV
- Carbonized Polyimide has somewhat higher SEY δ_{max} than other materials

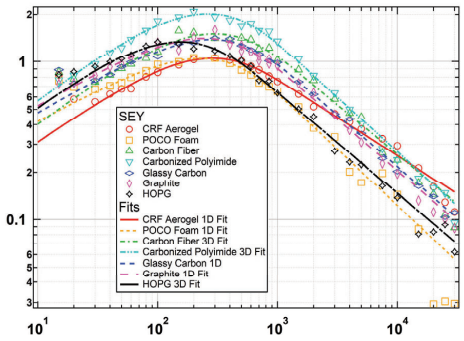
BSEY Yields

- All samples have BSEY >1000 eV that are similar to HOPG, which is a very low yield material
- Poco Foam and CRF Aerogel have BSEY <1000 eV that are lower than other materials
- Carbon Fiber and Carbonized Polyimide have BSEY <1000 eV that are somewhat higher than other materials

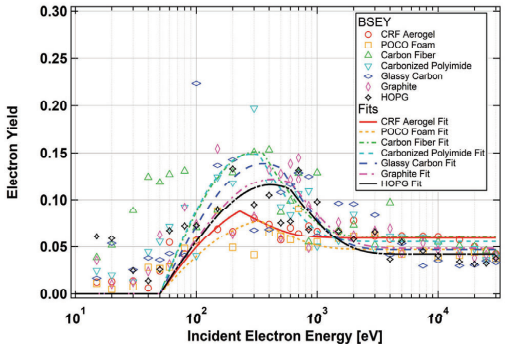
TEY Comparison



SEY Comparison



BSEY Comparison



NASA/GRC

Secondary Electron Suppression with Carbonized Aerogels

Intermediate Report

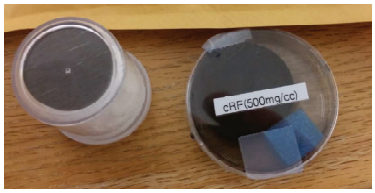
Sample Preparation and Characterization

Sample Photos
Electron Range
Sample Preparation
SEM/EDX Measurements
Optical Reflectivity Measurements

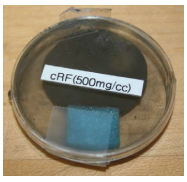
NASA/GRC Samples -- As Delivered 8/15/17



The left one is unlabeled; it is 1.010" (25.6 mm) diameter and 0.196" (4.97 mm) thick with rough surfaces that appear to show saw marks.







The right sample is labeled cRF (500mg/cc); it is approximately 1.390" (35.3 mm) diameter and 0.138" (3.47 mm) thick.

NASA/GRC Samples -- As Delivered 9/14/17

Glassy Carbon cRF Carbon Fiber Ordinary Carbon



Carbonized Polyimide Aerogel

P-120 Carbon Foam / Carbon Composite

Poco Foam

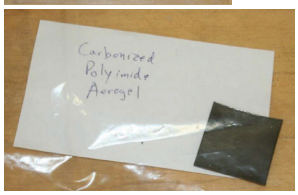
NASA/GRC Samples -- As Delivered 9/14/17



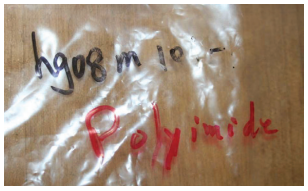
P-120 Carbon Foam / Carbon Composite

Poco Foam





Carbonized Polyimide Aerogel



hg08m10-Polyimide

Sample Thickness



Thickness Measurements

- Measurements made using a Mitutoyo micrometer (Model IP-65), with a resolution of ±1 μm.
- LAM samples were held in the calibrated USB calipers around the outer edge of the sample for thickness measurements.
- A total of six measurements were taken for each sample.
- Places at or near the outer contact spot were avoided when taking measurements.
- Measurements were entered into an Excel template that calculated the average, St. dev, St. dev of the mean, and fraction of uncertainty for each sample.

NASA/GRC

Secondary Electron Suppression with Carbonized Aerogels

Intermediate Report

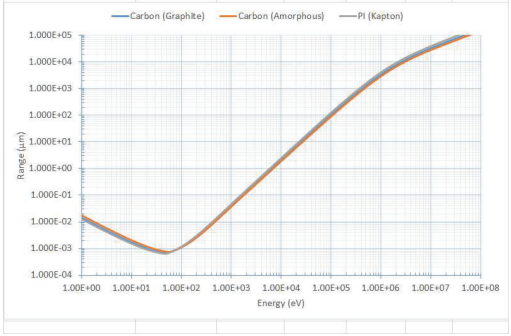
Sample Preparation and Characterization

Sample Photos
Electron Range
Sample Preparation
SEM/EDX Measurements
Optical Reflectivity Measurements

Relevant Materials Electron Range Curves

The maximum electron range is calculated from the input parameters listed in the table (stoichiometry, density, band gap) using the methods described in Wilson (see below). The range calculated in this way is typically about twice the penetration depth for electron at a given energy.

Material	Formula	Z	ρ(g/cm^3)	M (amu)	N_V	E_{gap} (eV)
Carbon (Graphite)	C (graphite)	6	1.7	12.01	3.06	0.1
Carbon (Amorphous)	C (amorphous/diam	6	2	12.011	3.117	0.5
PI (Kapton)	C22H10N2O5	5.01	1.42	9.769	2.568	2.32



Gregory Wilson and JR Dennison, "Approximation of Range in Materials as a Function of Incident Electron Energy," *IEEE Trans. on Plasma Sci.*, **40**(2), 305-310 (2012). DOI: 10.1109/TPS.2011.2176515

Anne Sterley, Gregory Wilson, Lisa Phillipps and JR Dennison, "Predictive Formula for Electron Penetration Depth of Diverse Materials over Large Energy Ranges," *Proceedings of the 14th Spacecraft Charging Technology Conference*, Space Research and Technology Centre of the European Space Agency (ESA/ESTEC), (Noordwyk, Netherlands, April 4-8, 2016), 2 pp.



Approximation of Range in Materials as a Function of Incident Electron Energy

Gregory Wilson and J. R. Dennison

Abstract—A simple composite analytic expression has been developed to approximate the electron range in materials. The expression is applicable over more than six orders of magnitude in energy (< 10 eV to > 10 MeV) and range ($10^{-8} - 10^{-2}$ m), with an uncertainty of $\leq 20\%$ for most conducting, semiconducting, and insulating materials. This is accomplished by fitting data from two standard NIST databases (ESTAR for the higher energy range and the electron inelastic mean free path (IMFP) for the lower energies). In turn, these data have been fit with well-established semi-empirical models for range and IMFP that are related to standard material properties (e.g., density, atomic number, atomic weight, stoichiometry, and bandgap energy). Simple relations between the IMFP and the range, based on the continuous-slow-down approximation, are used to merge results from the two databases into a composite range expression. A single free parameter, termed the effective number of valence electrons per atom N_v, is used to predict the range over the entire energy span.

Index Terms—Electron scattering, inelastic mean free path (IMFP), range, spacecraft charging.

Nomenclature

b	Stopping power proportionality constant.
c	Speed of light in vacuo.
CSDA	Continuous-slow-down approximation.
D	Dose rate.
$\overline{E}$	Mean energy lost per collision.
E_b	Electron beam energy.
E_{gap}	Bandgap energy.
E_{BH}, E_{LO}	Energies to determine n from the Bethe–Joy formula range extremes for NIST databases.
E_{min}	Energy at the minimum in the mean free path curve.
E_{max}	Energy at maximum secondary electron (SE) yield δ_{max}.
E_p^{eff}	Effective plasmon energy.
$\hbar$	Reduced Planck's constant.
J_b	Electron beam current density.
k	Empirical constant in the Bethe–Joy formula.
k_{RIC}	RIC proportionality constant.
M_A	Atomic weight.
m_e	Electron rest mass.
n	Stopping power exponent.
N_A	Avogadro's number.
N_v^{eff}	Effective number of valence electrons.
q_e	Electron charge.
R	Electron range (penetration depth).
RIC	Radiation-induced conductivity.
S_{CSDA}	Electron stopping power in CSDA.
v	Electron velocity.
Z_A	Atomic number.
β, γ, C, D, U	Coefficients used in the TPP-2M formula.
δ_{max}	Maximum SE yield.
Δ_{bs}	SE yield.
Δ	RIC power exponent.
ε_0	Permittivity of free space.
λ	Inelastic mean free path (IMFP) at $\overline{E}$.
λ_{SE}	SE IMFP.
λ_{EMFP}	EMFP.
λ_{min}	IMFP at E_{min}.
ρ_m	Mass density.
σ_{RIC}	Radiation-induced conductivity.

I. Introduction

THE RANGE R or maximum distance that an electron of a given incident energy can penetrate through a material before all kinetic energy is lost and the electron comes to rest is a common way to parameterize electron interactions with materials. The range is used in spacecraft charging calculations to predict the charge distribution of deposited electrons in materials and to model secondary and backscattered electron emission. It is also used to predict the distribution of energy deposited by incident electrons as they traverse a material; this distribution is further used to model RIC. It is therefore important for spacecraft charging models to have a realistic, reasonably accurate, and efficient expression to predict the approximate range of electron energies commonly encountered in space plasma fluxes, from ~ 10 eV to ~ 10 MeV. The expression needs to be readily implemented for a wide array of conducting, semiconducting, and insulating spacecraft materials with a minimal number of fitting parameters.

The Lichtenberg tree in Fig. 1 offers dramatic visual evidence of the validity of the range of electrons in a material. The white line seen at the center of the side view results from the melting of the PMMA plastic target during discharge, as electrons deposited in a narrow distribution at a depth of $R \approx 3$ mm by a monoenergetic ~ 1–MeV electron beam are released.

Manuscript received April 4, 2011; revised October 6, 2011 and November 9, 2011; accepted November 10, 2011. Date of publication January 10, 2012; date of current version February 10, 2012. This work was supported in part by the NASA Johns Webb Space Telescope Program through Goddard Space Flight Center, Greenbelt, MD, and in part by Utah State University Undergraduate Research and Creative Opportunities grant.

The authors are with the Materials Physics Group, Physics Department, Utah State University, Logan, UT 84322 USA (e-mail: GregoWilson@gmail.com; JR.Dennison@usu.edu).

Color versions of one or more of the figures in this paper are available online at http://ieeexplore.ieee.org.

Digital Object Identifier 10.1109/TPS.2011.2176515

0093-3813/$31.00 © 2012 IEEE

Electron Range Model

Simple model of the incident energy dependence of electron penetration depth in materials

Gregory Wilson and JR Dennison, "Approximation of Range in Materials as a Function of Incident Electron Energy," *IEEE Trans. on Plasma Sci.*, **40**(2), 305-310 (2012). DOI: 10.1109/TPS.2011.2176515

NASA/GRC

Secondary Electron Suppression with Carbonized Aerogels

Intermediate Report

Sample Preparation and Characterization

Sample Photos
Electron Range
Sample Preparation
SEM/EDX Measurements
Optical Reflectivity Measurements

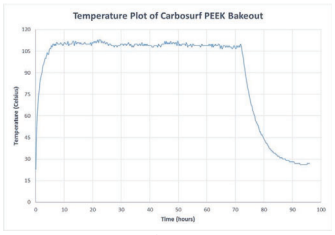
Sample Preparation and Treatment

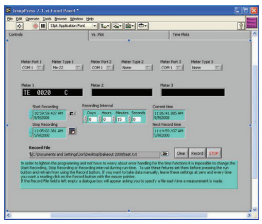
- All samples underwent the following preparation:
  - Cut to fit on sample blocks.
  - Ultrasonic cleaning in methanol
  - Baked out in $<10^{-3}$ Pa vacuum at ~110 °C for >48 hrs.
  - Stored in dry nitrogen glove box until they were put in test chamber
- The test chamber was:
  - Pumped down to $\sim10^{-7}$ Torr (takes ~3 days)
  - Tests performed at room temperature

All test samples will be provided by GRC. Details of the sample size and preparation will be determined through consultations between GRC and USU. Basic characterization measurements will be made of each sample including mass, density, and thickness. Examinations with optical microscopy and scanning electron microscopy will be made before and after electron emission tests. All samples will be characterized and will undergo vacuum bakeout at USU prior to any electron emission measurements.

Vacuum Bakeout Oven-Typical Results

ViaSat materials samples were subject to a vacuum bakeout prior to all measurements.



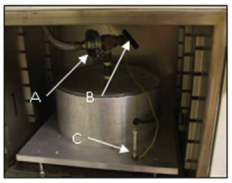


Vacuum Bakeout Specifications

- ~10 liter vacuum chamber mounted inside bakeout oven (Blue M Isallotherm Gravity Oven Model 70)
- Vacuum chamber pumped by mechanical/diffusion pump system to $<10^{-3}$ Pa. Equipped with (optional) cold trap. Pressure monitored with vacuum thermocouple and Bayard-Albert ionization gauges.
- Sample temperature maintained at ±1 K over room temperature to 525 K (250 ˚C).
- Temperature monitor with Type K thermocouple and recorded using a custom LabVIEW VI (front panel shown in figure).
- Typical bakeout is at 380 K (107 ˚C) and $5x10^{-4}$ Pa for ~72 hr.
- Typical plot of bakeout curve shown at left.

Vacuum Bakeout Oven-Instrumentation







(Left). Bake-out chamber, showing pumping station, oven, and computer.

(Top Right). Chamber in oven, showing: **(A)** vacuum connection, **(B)** main valve, **(C)** Type K thermocouple.

(Bottom Right). Chamber outside oven.

Sample Storage--Dry Nitrogen Glove Box



After Bakeout:

- Samples were then stored in a dry nitrogen gas filled glove box until they were used.

NASA/GRC

Secondary Electron Suppression with Carbonized Aerogels

Intermediate Report

Sample Preparation and Characterization

Sample Photos
Electron Range
Sample Preparation
SEM/EDX Measurements
Optical Reflectivity Measurements

Sample Preparation and Characterization

SEM/EDX Measurements of carbon samples

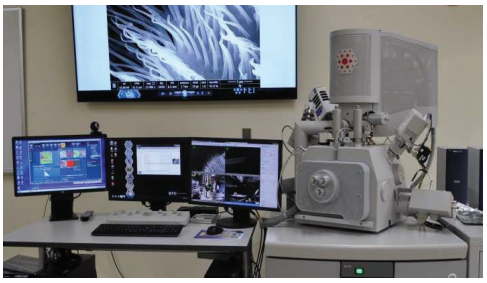
Objectives of SEM/EDX Measurements

- Explore surface morphology to help determine the effects of surface roughness on electron yields
- Measure chemical composition of sample surfaces with EDS
- Look for evidence of changes in surface chemistry with depth with energy dependent EDS measurements
- Look for mechanical damaged caused by shake tests

SEM/EDS Measurement Capabilities

SEM/EDS Analysis

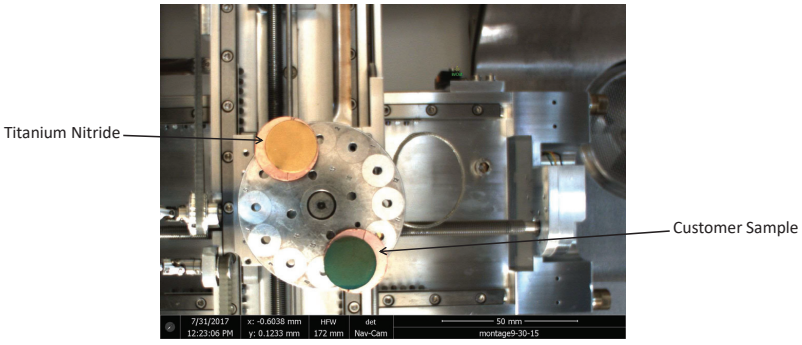
- FEI Quanta FEG 65 field-emission scanning electron microscope (FE-SEM)
- Structural analysis with resolution of ~3 nm
- Low vacuum and environmental modes available for samples susceptible to charging
- SEM measurements will provide information about surface roughness
- Energy dispersion spectroscopy (EDS) provides elemental analysis of near surface features and is useful for identification of contamination with elemental concentration resolution of ~0.3%
- Electron backscatter diffraction (EBSD) provides information about crystalline structure of the samples.



FEI Quanta FEG 65 field-emission scanning electron microscope (FE-SEM) at the USU Microscopy Core Facility.
http://rgs.usu.edu/microscopy/instruments/scanning-electron-microscope/

Sample Preparation and Characterization

SEM Measurements of samples



Samples shown mounted in SEM on carousel

Sample Preparation and Characterization

SEM /EDX Measurements of carbon samples

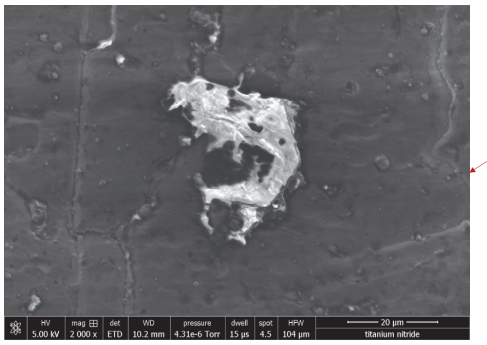
Summary of SEM Measurements and Results

- Six carbon samples studied plus a reference HOPG sample
- Data acquired
- SEM images taken in High Vacuum Mode using the ETD detector using various incident electron energies between 5-30 keV
- EDS measurements also taken for chemical composition at energies between 5-30 keV

Sample Preparation and Characterization

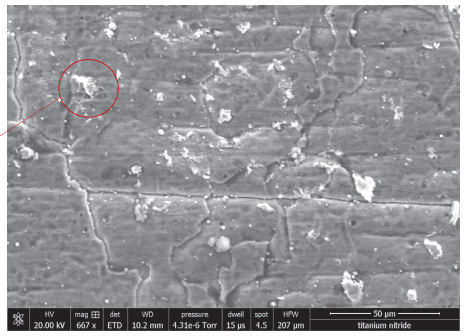
SEM /EDX Measurements of carbon samples

Titanium Nitride SEM Images



5 keV electrons, magnification of carbon spot

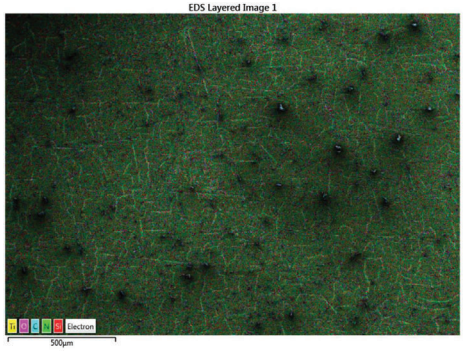
- 20 keV, magnification of cracks in surface



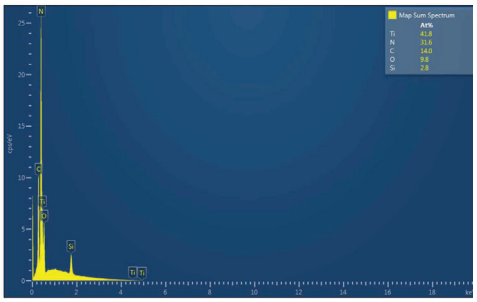
Sample Preparation and Characterization

SEM /EDX Measurements of carbon samples

Titanium Nitride ESD Images: 5 keV



- Mostly Ti and N in roughly equal parts, as you would expect.
- Some C, O and Si contamination
- Lowest energy (5 keV) is most surface sensitive

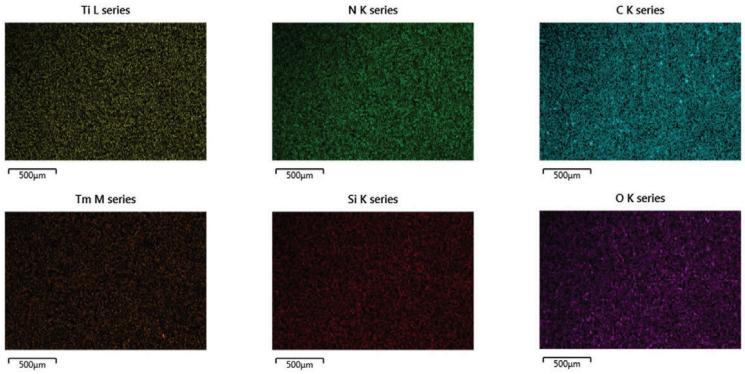


Sample Preparation and Characterization

SEM /EDX Measurements of carbon samples

Titanium Nitride ESD Elemental Maps: 5 keV

- Small spots are indeed carbon buildup on the surface



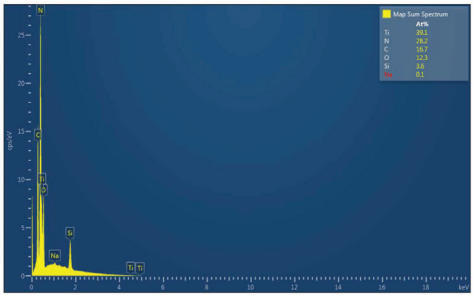
Sample Preparation and Characterization

SEM /EDX Measurements of carbon samples

Titanium Nitride ESD Images: 5 keV

- Higher magnification image of C spots
- Mostly Ti and N, as you would expect.
- Much more C contamination in particles
- Si and O also present





NASA/GRC

Secondary Electron Suppression with Carbonized Aerogels

Intermediate Report

Sample Preparation and Characterization

Sample Photos
Electron Range
Sample Preparation
SEM/EDX Measurements
Optical Reflectivity Measurements

Optical Transmission/Reflectivity

Measurements of optical transmission and reflectivity can be made using a fiber optic coupled deuterium/tungsten halogen light source (see Fig. 4). The reflectivity spectra will be made with a coupled pair of fiber optic UV/Vis/NIR spectrometers over a wavelength range of ~250 nm to ~1600 nm with a 0.5 nm to 3 nm resolution. A fiber optic-couple integrating sphere will be used for diffuse reflectivity measurements. A full analysis and error analysis will be provided.

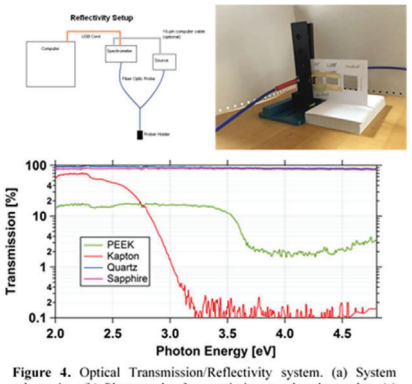


Figure 4. Optical Transmission/Reflectivity system. (a) System schematic. (b) Photograph of transmission stand and samples. (c) Typical optical transmission spectra.

NASA/GRC

Secondary Electron Suppression with Carbonized Aerogels

Intermediate Report

Electron Emission Test Results

Instrumentation

Yield Models

Electron Yield and Emission Spectra Measurements

Comparison with Previous Studies and literature values

Comparison of USU data for Yield standards (Au and HOPG graphite)

USU MPG Electron Emission Test Chamber

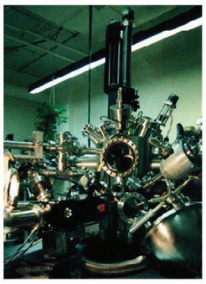
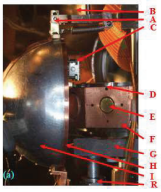


Figure 1. Electron Emission Test (EET) ultrahigh vacuum surface analysis chamber used for space environment simulation and charged particle scattering studies at Utah State University.



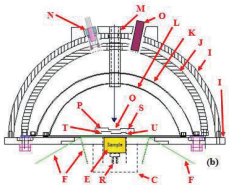


Figure. 2. Hemispherical Grid Retarding Field Analyzer (HGRFA). *(a) Photograph of sample stage and HGRFA detector (side view). (b) HGRFA cross section.*

LEGEND

A HGRFA Hinged Mount	*J HGRFA Collector*	*R Sample Current Lead*
B Sample Carousel/HGRFA Rotation Shaft	*K HGRFA Bias Grid*	*S SVP Faraday Cup*
C UHV Stepper Motor	*L HGRFA Inner Grid*	*T SVP 7 mm Diameter Au Electrode*
D Sample Block Faraday Cup	*M HGRFA Drift Tube*	*U SVP 3 mm Diameter Au Electrode*
E Sample (10 mm)	*N Electron Flood Gun*	*V SVP Wiring Channel*
F Sample Block	*O LED Light Source*	*W EPTP Vacuum Feedthrough*
G Cryogen Reservoir	*P Surface Voltage Probe (SVP)*	*X EPTP Wimacs Plate*
H HGRFA Face Plate	*Q Au Electron Emission Standard*	*Y Electrostatic Field Probe*
		Z Probe XYZ Translator

$$\sigma \equiv \frac{I_{SE}+I_{BSE}}{I_0} \equiv \frac{\int (I_{SE}+I_{BSE})\cdot dt}{\int I_0 \cdot dt} = \frac{I_c}{I_0} = \frac{CF \quad I_c}{I_c + I_z + I_{stg} + I_g(0V)}$$

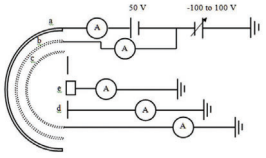


FIG. 3.2. Schematic of HGRFA.
(a) Solid hemispherical collector held at +50 V to attract all electrons that penetrate the bias grid. (b) Bias grid used to discriminate electron energies coming from within. (c) Inner grid used to provide a uniform electric field and shield from unwanted edge effects. (d) Sample stage comprises the hemispherical and sample mounting platform. (e) The sample is held in the center of hemisphere.

USU Pulsed Yield Electron Emission Test Chamber

The USU system for measuring electron emission uses a fully encased hemispherical grid retarding field analyzer (HGRFA) detector for full capture of the emitted electrons, with a retarding-field analyzer grid system for emitted electron energy discrimination [5,6]. Use of a HGRFA detector facilitates high-accuracy measurements of absolute yields on the order of ±2% for conducting samples and yields on insulators with errors of ±5%. [2,7]. It also allows the application of bias to each of the discrete elements of the detector [7]. These biases allow for the discrimination of secondary and backscatter electrons and the measurement of the electron emission spectra. A 0 V bias on the retarding grid allows all emitted electrons to be detected and the total yield to be measured. A −50 V bias applied to the retarding grid allows only the BSE to reach the detector, thus giving the BSE yield. The secondary yield is then determined as the difference of the total and BSE yield measurements. Full electron emission spectra can be obtained using the same apparatus, with the retarding grid stepping through a range of voltages [6].

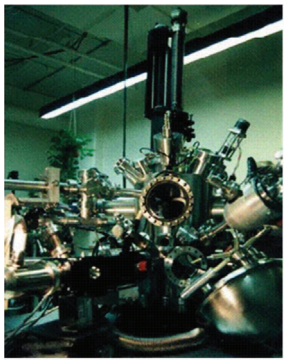
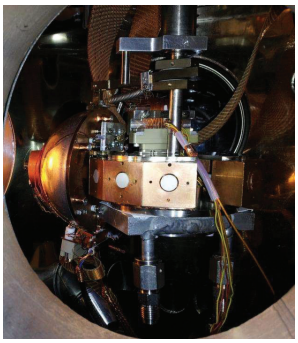
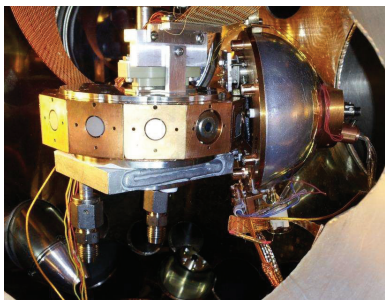


Figure 1. Electron Emission Test (EET) ultrahigh vacuum surface analysis chamber used for space environment simulation and charged particle scattering studies at Utah State University.

Sample Installation onto Carousel





NASA/GRC

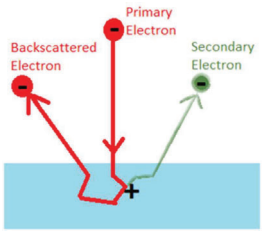
Secondary Electron Suppression with Carbonized Aerogels

Intermediate Report

Electron Emission Test Results

Instrumentation
Yield Models
Electron Yield and Emission Spectra Measurements
Comparison with Previous Studies and literature values
Comparison of USU data for Yield standards (Au and HOPG graphite)

Electron Yield Measurements



• Total yield is defined as the ratio of emitted electrons per incident electron, or

$$\sigma = \frac{Q_{out}}{Q_{in}}$$

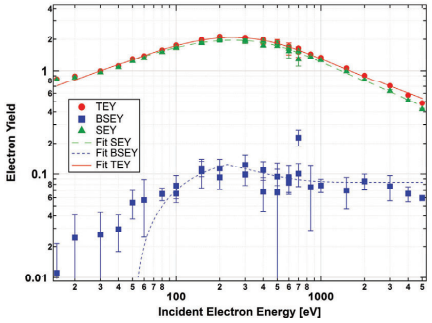
• Two other yields are defined for the two types of emitted electrons
  • Secondary electrons

$$\delta = \frac{Q_{SE}}{Q_{in}}$$

  • Backscattered electrons

$$\eta = \frac{Q_{BSE}}{Q_{in}}$$

Simple 1D Yield Model Fitting Functions



SEY Yield Model

1D SEY Model

$$\delta(E) := \frac{E^{m-n}}{2\cdot\varepsilon\cdot\gamma}\cdot\left(1 - e^{-\gamma\cdot E^{n}}\right)$$

Parameters:
m- left slop on a log graph
(m-n)- right slope on a log graph
ε- vertical shift of left side on a log graph
γ- vertical shift of right side on a log graph

BSEY Yield Model

BSEY 3Param Fit

$$\eta(E_0) := \begin{cases} 0 & if\ E_0 \le 50\ eV \\ \frac{\log\left(\frac{E_0}{50\ eV}\right)}{\log\left(\frac{E_{max}}{50\ eV}\right)}\cdot\left[(\eta_{max}-\eta_0)\cdot e^{\frac{-(E_0-E_{max})}{E_{max}}}+\eta_0\right] & if\ 50\ eV < E_0 \le E_{max} \\ \left[(\eta_{max}-\eta_0)\cdot e^{\frac{-(E_0-E_{max})}{E_{max}}}+\eta_0\right] & if\ E_{max} < E_0 \end{cases}$$

Parameters
E_{max}- energy of max BSEY
mix- maximum BSEY
η_0- asymptotic BSEY for large incident energies.

Other SEY Models

- SEY3DFit
- Sternglass
- Dionne
- Hastings
- Feldman

$$f(E) = \frac{E^{m-n}}{2\cdot\varepsilon\cdot\gamma}\cdot\left(\frac{1}{2} - \text{expint}\left(3,\gamma\cdot E^{n}\right)\right)$$

$$f(E) = \frac{\delta_{.max}\cdot E}{E_{.max}}\cdot e^{2-2\cdot\left(\frac{E}{E_{.max}}\right)^{.5}}$$

$$f(E) = \frac{B}{\alpha}\cdot 1.35\cdot E^{-.35}\cdot\left(1-e^{\frac{-\alpha}{1.35}E^{1.35}}\right)$$

$$f(E) = 1.114\cdot\delta_{.max}\left(\frac{E_{.max}}{E}\right)^{.35}\cdot\left[1 - e^{-2.28\cdot\left(\frac{E}{E_{.max}}\right)^{1.35}}\right]$$

$$f(E) = \frac{1}{1-e^{-c2}}\cdot\delta_{.max}\left(\frac{E_{.max}}{E}\right)^{\left(\frac{1-e^{-c2}}{1-e^{-c2}-c2\cdot e^{-c2}}\right)\cdot 1}\cdot\left[1-e^{-c2\left(\frac{E}{E_{.max}}\right)^{\frac{1-e^{-c2}}{1-e^{-c2}-c2\cdot e^{-c2}}}}\right]$$

NASCAP BSEY Model

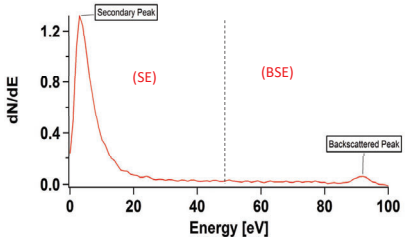
$$f(E) = \begin{cases} 0 \text{ if } E \le 50\text{eV} \\ \left[\frac{\log\left(\frac{E}{50\text{eV}}\right)}{\log\left(\frac{1000\text{eV}}{50\text{eV}}\right)} \cdot \left(.1 \cdot e^{\frac{-E}{5000\text{eV}}} + \eta_{.0}\right)\right] \text{ if } E \le 1000\text{eV} \\ .1 \cdot e^{\frac{-E}{5000\text{eV}}} + \eta_{.0} \text{ if } E > 1000\text{eV} \end{cases}$$

This model only has one free parameter and doesn't fit most BSEY data very well.

The 3 Parameter BSEY model was developed to allow us to fit more BSEY data.

Emitted Energy Distribution

- Electrons are differentiated by their origin from a theoretical point of view.
  - BSE originate as primary incident electrons.
  - SE originate from within the material.
- Empirically, emitted electrons are differentiated by measuring their kinetic energies. By convention:
  - SE <50 V
  - BSE > 50 eV.



- SE are fit with the Chung-Everhart model
- BSE are fit as a gaussian, centered at the incident energy, *Eoh*.

Emitted Energy Distribution

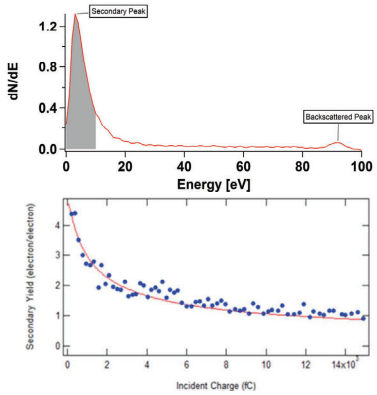
- Chung-Everhart model for SE energy distribution

  $(den/DE)_{SE}(E) = A \cdot (E - E_0) / ((E - E_0) + X)^4$

- Gaussian function fit for BSE energy distribution

  $(den/DE)_{BSE}(E) = y_0 + Apex(-((E-E_0)/\Delta E)^2)$

- Measuring the emitted electron energy distribution allows us to model the evolution of electron yield for varying surface potentials (*i.e.* for insulators, or floating conductors).



NASA/GRC

Secondary Electron Suppression with Carbonized Aerogels

Intermediate Report

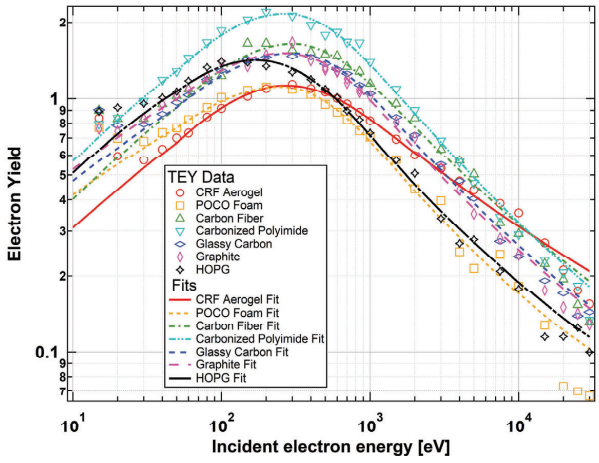
Electron Emission Test Results

Instrumentation
Yield Models
Electron Yield and Emission Spectra Measurements
Comparison with Previous Studies and literature values
Comparison of USU data for Yield standards (Au and HOPG graphite)

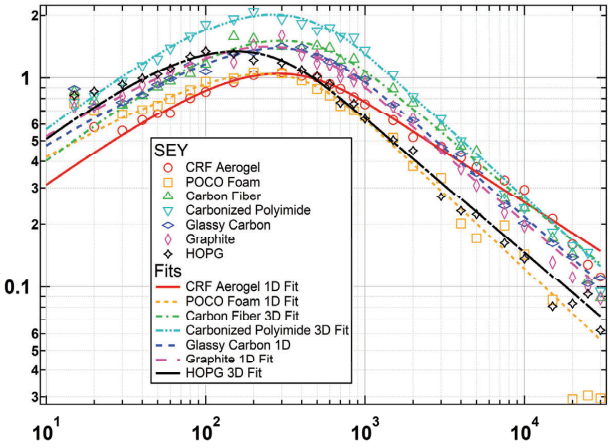
Yield Measurements

- Yield measurements were made:
  - using 10 electron beam pulses (3 μs) per beam energy
  - integrating the incident and emitted charges
  - combining results using equations from slide 38.
- Conservative uncertainties (precision) were estimated using the standard deviation of the 10 pulses for each energy.

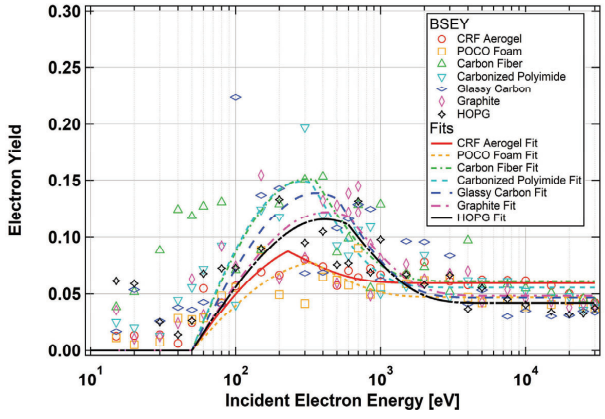
TEY Comparison



SEY Comparison



BSEY Comparison



Yield Features

		CRF Aerogel	POCO Foam	Glassy Carbon	Graphite	Carbon Fiber	Carbonized Polyimide	HOPG
TEY	σMax	1.14 ± 0.02	1.12 ± 0.02	1.5 ± 0.2	1.5 ± 0.1	1.7 ± 0.2	2.2 ± 0.1	1.42 ± 0.05
	Emax	280 ± 50	240 ± 30	280 ± 50	260 ± 50	300 ± 80	270 ± 50	170 ± 50
	E1	135 ± 5	97 ± 5	56 ± 3	46 ± 5	46 ± 4	30 ± 2	40 ± 2
	E2	610 ± 10	440 ± 20	1060 ± 30	1000 ± 30	1400 ± 100	1690 ± 80	610 ± 20
SEY	δMax	1.06 ± 0.04	1.04 ± 0.02	1.4 ± 0.2	1.4 ± 0.1	1.5 ± 0.2	2.2 ± 0.1	1.3 ± 0.1
	Emax	280 ± 50	230 ± 40	280 ± 50	240 ± 50	300 ± 80	270 ± 50	160 ± 50
	E1	180 ± 20	140 ± 10	62 ± 4	50 ± 5	69 ± 10	30 ± 2	42 ± 2
	E2	470 ± 30	370 ± 40	930 ± 70	850 ± 50	1200 ± 200	1690 ± 80	510 ± 40
BSEY	η0	0.059 ± 0.004	0.047 ± 0.005	0.047 ± 0.014	0.048 ± 0.01	0.06 ± 0.02	0.055 ± 0.015	0.042 ± 0.009
	ηMax	0.088 ± 0.007	0.078 ± 0.007	0.13 ± 0.02	0.118 ± 0.01	0.15 ± 0.02	0.15 ± 0.02	0.11 ± 0.01
	Ema	230 ± 50	340 ± 100	500 ± 160	600 ± 140	350 ± 120	350 ± 120	600 ± 140

Yield Fits

Shaded cells are the best fits according to the chi square test. The NASCAP fitting tool calculates chi square values differently than the routine used for all other fits. Therefore, these values are not included since they are not comparable.

			CRF Aerogel	POCO Foam	Glassy Carbon	Graphite	Carbon Fiber	Carbonized Polyimide	HOPG
Chi Square	UV	1D	0.0128	0.0189	0.0237	0.099	0.102	0.113	0.0413
		3D	0.0143	0.0191	0.0251	0.101	0.0973	0.0958	0.0367
		Stern glass	0.677	0.301	0.638	0.809	0.804	0.979	0.488
		Dionne	0.151	0.33	0.505	0.711	0.52	1.06	0.384
		Hastings	0.151	0.33	0.505	0.711	0.52	1.06	0.384
		Feldman	0.345	0.215	0.384	0.578	0.363	0.643	0.223
	REKP	Nascap	0.015	0.0154	0.0671	0.0421	0.0939	0.0501	0.0328
		b Param	0.00445	0.0072	0.0498	0.0261	0.067	0.0187	0.0201
IEYFits	1D	m	0.53 ± 0.03	0.41 ± 0.03	0.45 ± 0.02	0.44 ± 0.04	0.51 ± 0.05	0.51 ± 0.03	0.38 ± 0.03
		n	1.02 ± 0.02	1.13 ± 0.03	1.1 ± 0.02	1.09 ± 0.04	1.13 ± 0.04	1.18 ± 0.03	1.07 ± 0.03
		x	5.4 ± 0.6	3.1 ± 0.4	2.9 ± 0.3	2.6 ± 0.4	3.7 ± 0.7	2.7 ± 0.4	1.8 ± 0.2
		y	0.0042 ± 0.0004	0.0019 ± 0.0004	0.0019 ± 0.0003	0.0024 ± 0.0006	0.0018 ± 0.0004	0.0014 ± 0.0003	0.0037 ± 0.0007
	3D	m	0.41 ± 0.03	0.48 ± 0.03	0.52 ± 0.03	0.5 ± 0.04	0.58 ± 0.05	0.58 ± 0.03	0.45 ± 0.03
		n	1.1 ± 0.02	1.21 ± 0.03	1.19 ± 0.02	1.17 ± 0.04	1.21 ± 0.04	1.27 ± 0.03	1.15 ± 0.03
		x	6.7 ± 0.8	3.7 ± 0.5	3.6 ± 0.4	3.1 ± 0.5	4.6 ± 1	3.3 ± 0.4	2.1 ± 0.2
		y	0.0016 ± 0.0002	0.00067 ± 0.00014	0.0007 ± 0.0001	0.0009 ± 0.0002	0.00064 ± 0.00017	0.0005 ± 0.0001	0.0014 ± 0.0003
	Sternglass	Emax[eV]	350 ± 40	250 ± 20	310 ± 20	260 ± 20	350 ± 30	290 ± 20	190 ± 10
		δMax	1.11 ± 0.05	1.12 ± 0.04	1.47 ± 0.05	1.5 ± 0.05	1.58 ± 0.06	2.11 ± 0.07	1.4 ± 0.05
	Dionne	b	0.0142 ± 0.0009	0.019 ± 0.002	0.021 ± 0.002	0.024 ± 0.002	0.02 ± 0.002	0.031 ± 0.003	0.033 ± 0.003
		w	0.0024 ± 0.0002	0.0038 ± 0.0005	0.0029 ± 0.0003	0.0033 ± 0.0003	0.0025 ± 0.0002	0.0031 ± 0.0003	0.0058 ± 0.0007
	Hastings	Emax[eV]	200 ± 10	140 ± 10	180 ± 10	160 ± 10	200 ± 10	170 ± 10	104 ± 9
		δMax	1.12 ± 0.03	1.08 ± 0.04	1.45 ± 0.05	1.5 ± 0.05	1.56 ± 0.05	2.06 ± 0.07	1.34 ± 0.04
	Feldman	Emax[eV]	210 ± 10	170 ± 10	200 ± 10	180 ± 10	220 ± 10	190 ± 10	123 ± 7
		δMax	1.14 ± 0.03	1.18 ± 0.04	1.55 ± 0.06	1.61 ± 0.06	1.67 ± 0.06	2.25 ± 0.07	1.45 ± 0.04
		c2	2.2 ± 0.08	1.93 ± 0.09	2 ± 0.1	2 ± 0.1	2 ± 0.09	1.94 ± 0.08	1.95 ± 0.08
	Reknap	δMax	1.12	1.06	1.38	1.48	1.5	2.02	1.31
		Emax[eV]	0.189	0.151	0.251	0.2	0.236	0.218	0.12
		RC1	0.681	0.684	1.2	0.648	0.794	1.09	0.427
		RExp1	0.498	0.634	0.599	0.44	0.498	0.711	0.561
		RC2	1	1	1	1	1	1	1
		RExp2	1.52	1.77	1.86	1.76	1.66	1.84	1.72
BSEYFits	Reknap	η0	0.021 ± 0.006	0.01 ± 0.006	0.03 ± 0.01	0.032 ± 0.008	0.04 ± 0.015	0.03 ± 0.01	0.023 ± 0.009
	3Param	ηMax	0.087 ± 0.007	0.078 ± 0.007	0.13 ± 0.02	0.12 ± 0.01	0.15 ± 0.02	0.15 ± 0.01	0.11 ± 0.01
		Emax[eV]	230 ± 50	340 ± 100	500 ± 160	600 ± 140	350 ± 120	330 ± 60	600 ± 140
		η0	0.059 ± 0.004	0.047 ± 0.005	0.047 ± 0.014	0.05 ± 0.01	0.061 ± 0.015	0.055 ± 0.008	0.042 ± 0.009

Emission Spectra Fits

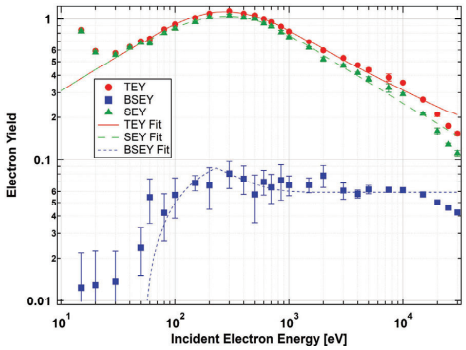
		CRF Aerogel	POCO Foam	Glassy Carbon	Graphite	Carbon Fiber	Carbonized Polyimide	HOPG
Chung Everhart SE Distribution	A	113 ± 5	110 ± 4	87 ± 11	132 ± 10	230 ± 10	120 ± 10	153 ± 7
	χ	4.62 ± 0.08	4.6 ± 0.06	4.5 ± 0.2	5 ± 0.2	6.5 ± 0.1	4.7 ± 0.2	5.36 ± 0.09
	Eoffset	1.1 ± 0.02	± 0.02	1.13 ± 0.08	1.29 ± 0.04	1.22 ± 0.03	1.57 ± 0.06	0.92 ± 0.02
Gaussian Fit BSE Distribution	Yoffset	0.0011 ± 0.0004	0.0008 ± 0.0003	0 ± 0.002	0.0008 ± 0.0004	0.0015 ± 0.0004	0.0011 ± 0.0003	0.0015 ± 0.0007
	A	0.0141 ± 0.0008	0.0148 ± 0.0005	0.041 ± 0.002	0.014 ± 0.0007	0.0175 ± 0.0008	0.0107 ± 0.0007	0.0141 ± 0.0012
	Ebeam	53.7 ± 0.1	53.78 ± 0.07	53.2 ± 0.1	53.68 ± 0.1	54.2 ± 0.08	53.6 ± 0.1	53.68 ± 0.16
	Width	2.4 ± 0.2	2.5 ± 0.1	3.8 ± 0.3	2.6 ± 0.2	2.2 ± 0.1	2.3 ± 0.2	2.6 ± 0.3

CRF Aerogel Yield Results

TEY Features:
E_1=135 ± 5 eV
E_2=610 ± 10eV
E_{max}=280 ± 50 eV
σ_{max}=1.14 ± 0.02

SEY Features:
E_1=180 ± 20 eV
E_2=470 ± 30eV
E_{max}=280 ± 50 eV
δ_{max} =1.06 ± 0.04

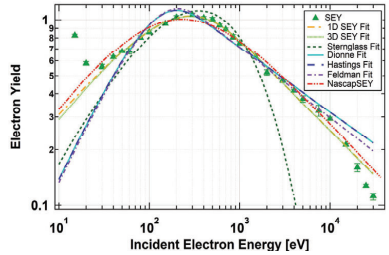
Best Fits
SEY 1D
BSEY 3 Parameter

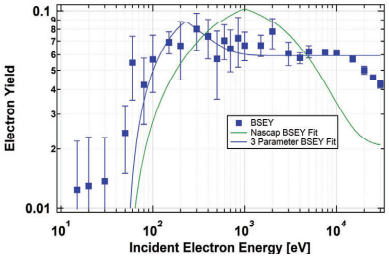


CRF Aerogel Fits Performed

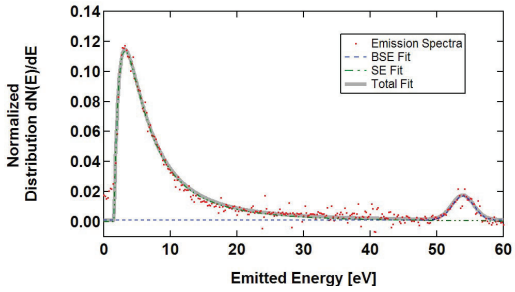
	SEY ChiSq
SEY 1D	0.0128
SEY 3D	0.0143
Sternglass	0.677
Dionne	0.151
Hastings	0.151
Feldman	0.145

	BSEY ChiSq
BSEY Nascap	0.0150
BSEY 3 Parameter	0.00445





CRF Aerogel Energy Distribution



Chung-Everhart Fit (SE Distribution)

A	= 113 ± 5
X	= 4.62 ± 0.08
E_0	= 1.10 ± 0.02

Gaussian Fit (BSE Distribution)

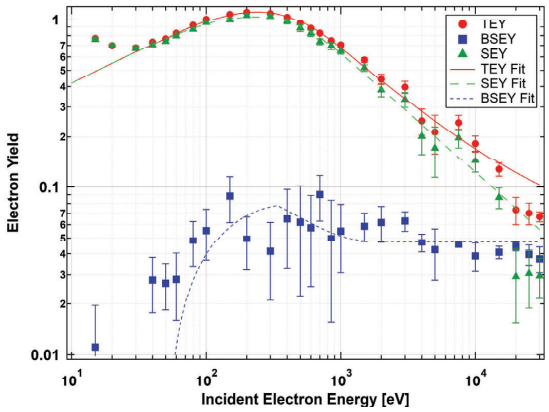
y_0	= 0.0011 ± 0.0004
A	= 0.0141 ± 0.0008
E_0	= 53.7 ± 0.1
width	= 2.4 ± 0.2

Poco Foam Yield Results

TEY Features:
E_1=97 ± 5 eV
E_2=440 ± 20eV
E_{max}=240 ± 30 eV
σ_{max}=1.12 ± 0.02

SEY Features:
E_1=140 ± 10 eV
E_2=370 ± 40eV
E_{max}=230 ± 40 eV
δ_{max} =1.04 ± 0.02

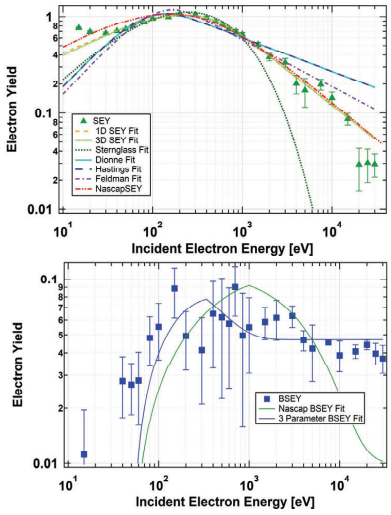
Best Fits
SEY 1D
BSEY 3 Parameter



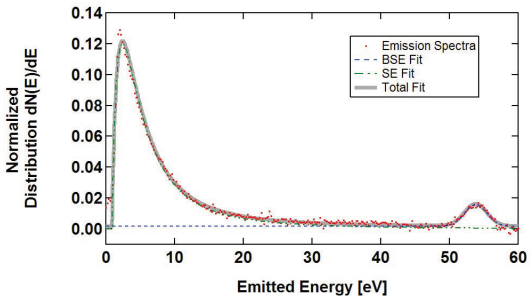
POCO Foam Fits Performed

	SEY ChiSq
SEY 1D	0.0189
SEY 3D	0.0191
Sternglass	0.301
Dionne	0.330
Hastings	0.330
Feldman	0.215

	BSEY ChiSq
BSEY Nascap	0.0154
BSEY 3 Parameter	0.00720



Poco Foam Energy Distribution



Chung-Everhart Fit (SE Distribution)

A	= 110 ± 4
X	= 4.60 ± 0.06
E_0	= 0.87 ± 0.02

Gaussian Fit (BSE Distribution)

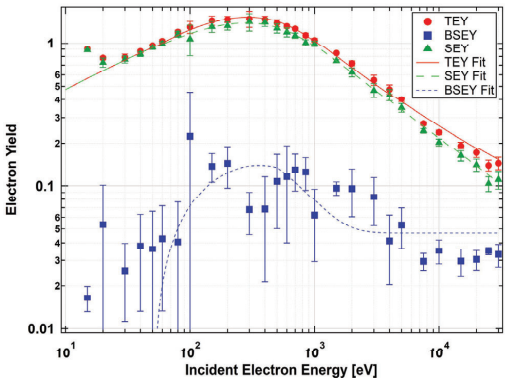
y_0	= 0.0008 ± 0.0003
A	= 0.0148 ± 0.0005
E_0	= 53.78 ± 0.07
width	= 2.5 ± 0.1

Glassy Carbon Yield Results

TEY Features:
E_1 = 56 ± 3 eV
E_2 = 1060 ± 30 eV
E_{max} = 290 ± 40 eV
σ_{max} = 1.5± 0.2

SEY Features:
E_1 = 62 ± 4 eV
E_2 = 930 ± 70 eV
E_{max} = 280 ± 50 eV
δ_{max} = 1.4 ± 0.2

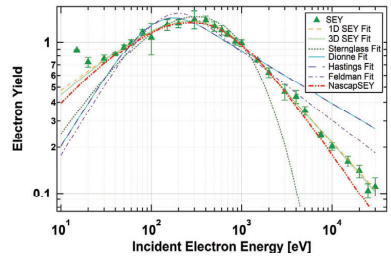
Best Fits
SEY 1D
BSEY 3 Parameter

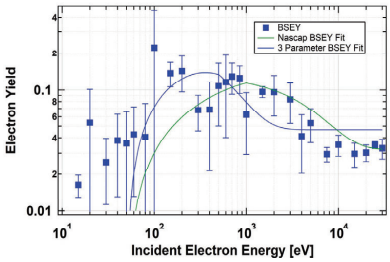


Glassy Carbon Fits Performed

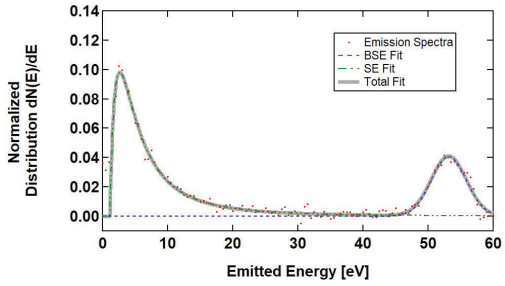
	SEY ChiSq
SEY 1D	0.0237
SEY 3D	0.0251
Sternglass	0.638
Dionne	0.505
Hastings	0.505
Feldman	0.384

	BSEY ChiSq
BSEY Nascap	0.0671
BSEY 3 Parameter	0.0498





Glassy Carbon Energy Distribution



Chung-Everhart Fit (SE Distribution)

A	= 87 ± 11
X	= 4.5 ± 0.2
E_0	= 1.13 ± 0.08

Gaussian Fit (BSE Distribution)

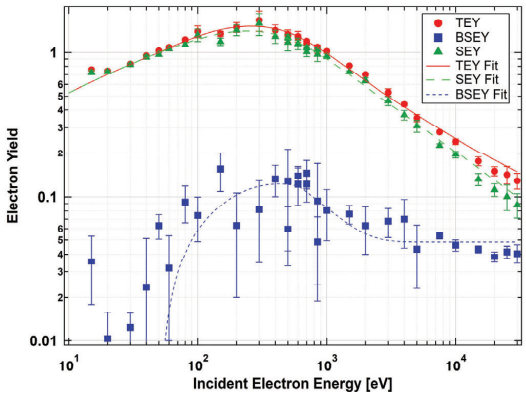
y_0	= 0.000 ± 0.002
A	= 0.041 ± 0.002
E_0	= 53.2 ± 0.1
width	= 3.8 ± 0.3

Ordinary Graphite Yield Results

TEY Features:
E_1 = 46 ± 5 eV
E_2 = 1000 ± 30 eV
E_{max} = 260 ± 50 eV
σ_{max} = 1.5 ± 0.1

SEY Features:
E_1 = 50 ± 5 eV
E_2 = 850 ± 50 eV
E_{max} = 240 ± 50 eV
δ_{max} = 1.4 ± 0.1

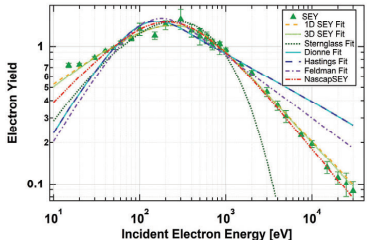
Best Fits
SEY 1D
BSEY 3 Parameter

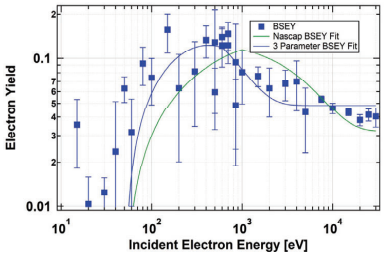


Ordinary Graphite Fits Performed

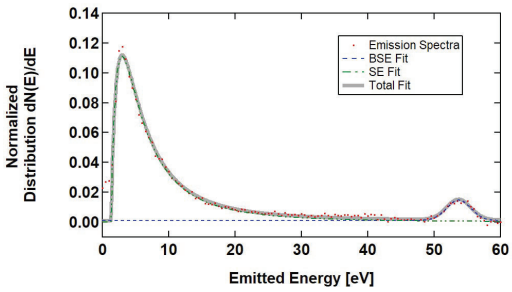
	SEY ChiSq
SEY 1D	0.0999
SEY 3D	0.101
Sternglass	0.809
Dionne	0.711
Hastings	0.711
Feldman	0.578

	BSEY ChiSq
BSEY Nascap	0.0421
BSEY 3 Parameter	0.0261





Ordinary Graphite Energy Distribution



Chung-Everhart Fit (SE Distribution)

A = 132 ± 10

X = 5.0 ± 0.2

E_0 = 1.29 ± 0.04

Gaussian Fit (BSE Distribution)

y_0 = 0.0008 ± 0.0004

A = 0.0140 ± 0.0007

E_0 = 53.68 ± 0.10

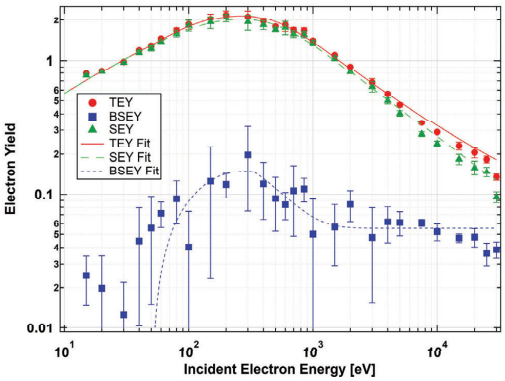
width = 2.6 ± 0.2

Carbonized Polyimide Yield Results

TEY Features:
E_1 = 30 ± 2 eV
E_2 = 1690 ± 80 eV
E_{max} = 270 ± 50 eV
σ_{max} = 2.2 ± 0.1

SEY Features:
E_1 = 30 ± 2 eV
E_2 = 1560 ± 80 eV
E_{max} = 270 ± 50 eV
δ_{max} = 2.0 ± 0.1

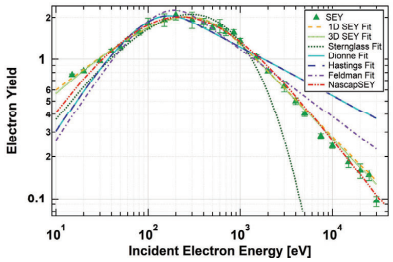
Best Fits
SEY 3D
BSEY 3 Parameter

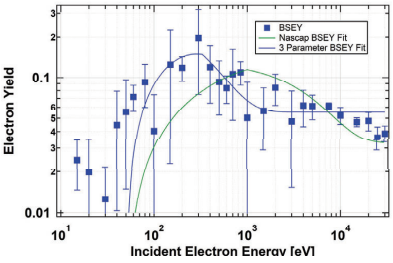


Carbonized Polyimide Fits Performed

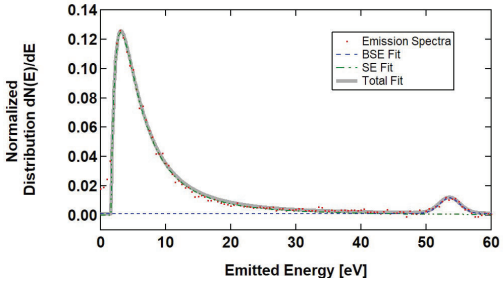
	SEY ChiSq
SEY 1D	0.113
SEY 3D	0.0958
Sternglass	0.979
Dionne	1.06
Hastings	1.06
Feldman	0.643

	BSEY ChiSq
BSEY Nascap	0.0501
BSEY 3 Parameter	0.0187





Carbonized Polyimide Energy Distribution



Chung-Everhart Fit (SE Distribution)

A	= 120 ± 10
X	= 4.7 ± 0.2
E_0	= 1.57 ± 0.06

Gaussian Fit (BSE Distribution)

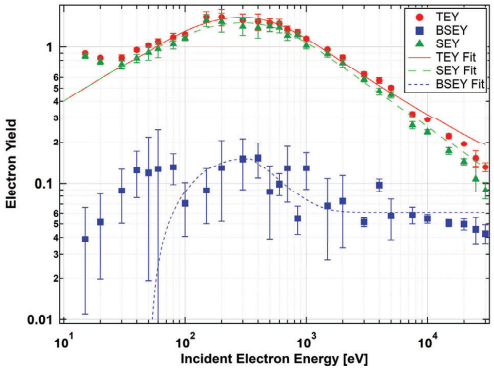
y_0	= 0.0011 ± 0.0003
A	= 0.0107 ± 0.0007
E_0	= 53.6 ± 0.1
width	= 2.3 ± 0.2

Carbon Fiber Yield Results

TEY Features:
E_1 = 46 ± 4 eV
E_2 = 1400 ± 100 eV
E_{max} = 300 ± 80 eV
σ_{max} = 1.7 ± 0.2

SEY Features:
E_1 = 69 ± 10 eV
E_2 = 1200 ± 200 eV
E_{max} = 300 ± 80 eV
δ_{max} = 1.5 ± 0.2

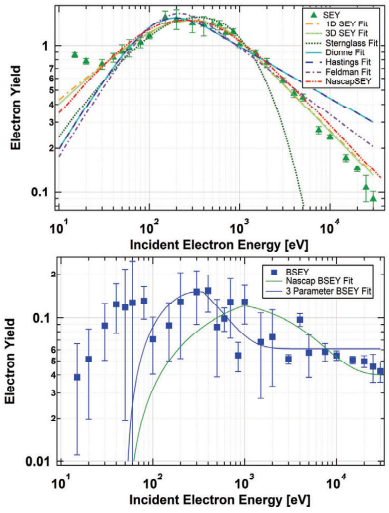
Best Fits
SEY 3D
BSEY 3 Parameter



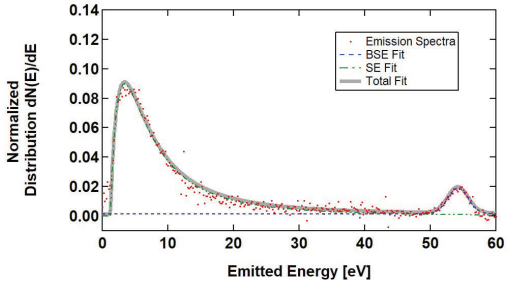
Carbon Fiber Fits Performed

	SEY ChiSq
SEY 1D	0.102
SEY 3D	0.0973
Sternglass	0.804
Dionne	0.520
Hastings	0.520
Feldman	0.363

	BSEYChiSq
BSEY Nascap	0.0939
BSEY 3 Parameter	0.0670



Carbon Fiber Energy Distribution



Chung-Everhart Fit (SE Distribution)

A	= 230 ± 10
X	= 6.5 ± 0.1
E_0	= 1.22 ± 0.03

Gaussian Fit (BSE Distribution)

γ_0	= 0.0015 ± 0.0004
A	= 0.0175 ± 0.0008
E_0	= 54.20 ± 0.08
width	= 2.2 ± 0.1

NASA/GRC

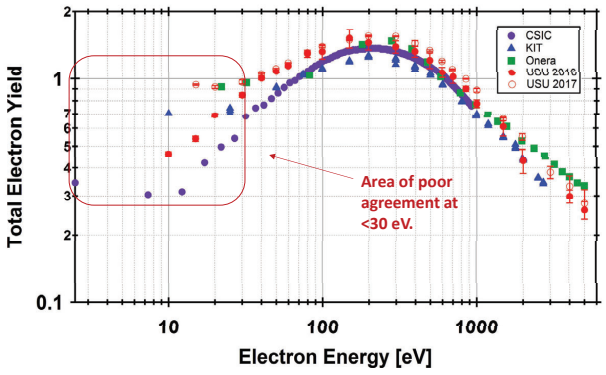
Secondary Electron Suppression with Carbonized Aerogels

Intermediate Report

Electron Emission Test Results

Instrumentation
Yield Models
Electron Yield and Emission Spectra Measurements
Comparison with Previous Studies and literature values
Comparison of USU data for Yield standards (Au and HOPG graphite)

Round Robin Comparison of HOPG Graphite Data



- **HOPG data have been compared with data taken by other laboratories in a Round Robin test and show that Agreement between data from different labs is good above ~30-50 eV.**
- **Values agree within ~10% above 200 eV and ~20 % down to ~30 eV.**
- **USU data may be noisy due to low yield or to negative charging. Yield values <30 eV may be higher than actual values due to stage bias.**

JR Dennison, Justin Christensen, Justin Dekany, Clint Thomson, Neal Nickles, Robert E. Davies, Mohamed Belhaj, Kazuhiro Toyoda, Arifur R. Khan, Kazutaka Kawasaki, Shunsuke Inoue, Isabel Montero, María E. Dávila and Leandro Olano, "Absolute Electron Emission Calibration: Round Robin Tests of Au and Polyimide," *Proceedings of the* 14th *Spacecraft Charging Technology Conference*, Space Research and Technology Centre of the European Space Agency (ESA/ESTEC), (Noordwijk, Netherlands, April 4-8, 2016) , 7 p.

Summary of Comparison of USU and Literature Values for Carbon

- This section compares results from different sources on their work with Carbon.

Comparison of USU and Literature SEY Values for Carbon

Table 7.2 Comparison of SE yield measurements of graphitic carbon

Reference	Conditions	Parameters				SE Yield at Incident Beam Energy (keV)										
		δ_{max}	E_{max} (keV)	$E_{1\sigma}$ (keV)	$E_{2\sigma}$ (keV)	0.1	0.2	0.3	0.5	1.0	1.5	2.0	2.5	3.0	5.0	10.0
MPG SEE Work	Graphite, (pyrolytic HOPG)	1.21	0.210	0.113	0.312	0.85	1.01	1.05	0.88	0.79					0.231	0.132
MPG SEE Work	Graphite, microcrystallins (Aquadag[TM])	1.35	0.240	0.099	0.418	1.10	1.41	1.28	1.14	0.856					0.266	0.140
MPG SEE Work	Graphitic amorphous carbon	1.73	0.243	0.077	0.820	1.44	1.67	1.69	1.37	0.886					0.246	0.210
Boergeler, 1993									0.155	0.990	0.68	0.527	0.442	0.400	0.315	
Bronstein, 1969		0.85	0.30	none	none	0.709	0.82	0.85	0.79	0.543		0.308		0.209		
Bruining, 1938	Graphite, microcrystallins (Aquadag[TM])	1.02	0.300	0.240	0.560	0.77	0.95	1.02	0.90							
Bruining, 1938	Graphite, Turbostatic carbon (soot)	0.47	0.45	none	None	0.3	0.40	0.42	0.46							
Caron, 1998	Graphitic carbon	2.2	0.275	0.200	1.100	1.0	2.0	2.0	1.81	0.97	0.72	0.62	0.50	0.40	0.25	
Caron, 1998	Disordered carbon (sputtered)	1.1	0.275	0.250	0.300	0.48	0.98	1.0	0.90	0.58	0.43	0.37	0.28	0.23	0.10	
Farhang, 1993	Disordered graphitic carbon (pocographite)	0.54	0.30	none	none	0.29	0.51	0.54	0.49	0.38						
Kanaya, 1972																
Kanaya, 1934				0.35											0.211	0.143
Kanter, 1961,								0.90							0.501	
Moncrieff, 1976													0.334			
Reimer, 1980										1.56						
Rothwell, 1988		1.10	0.30	0.25	0.50		0.92	1.10	1.02	0.72	0.39	0.36		0.33		
Rumi, 1982	Graphite, microcrystallins (Aquadag[TM])	0.91	0.250	none	none		0.89	0.86	0.70	0.50	0.43					
Rumi, 1982	Graphite, Turbostatic carbon with hydrogen (Ghrytol[TM])	0.88	0.247	none	none		0.78	0.89	0.62	0.39	0.38					
Rumi, 1982	Graphite, Turbostatic carbon (ED lamp black, soot)	0.88	0.250	none	none		0.82	0.82	0.62	0.43	0.42					
Rumi, 1982	Graphite (AT panels)	0.89	0.270	none	none											
Stemglass, 1954	Graphite, microcrystallins (Aquadag[TM])	1.27														
Stemglass, 1954	Amorphous carbon, hydrogenated															
Whetten, 1965	Graphite (pyrolytic)	1.0	0.310	0.310	0.310						0.45	0.40	0.33			
Wintucky, 1981	Graphite (pyrolytic)			<0.20	0.33		1.17	1.03	0.83	0.57	0.45	0.44				
Wintucky, 1981	Graphite, disordered (sputtered pyrolytic)	0.42	0.400	none	none				0.41	0.34	0.32	0.31				
Wintucky, 1981	Graphite, Turbostatic carbon (soot)	0.4	0.450	none	none			0.39	0.37	0.35	0.42	0.44				
Wittry, 1966															0.17	
	(pocographite)															
Woods,1985,1987	Disordered graphitic carbon (pocographite, sputtered)	0.53	0.29	none	none	0.50	0.53	0.55	0.48	0.41	0.32	0.29				
Woods,1985,1987	Graphite	1.12	0.22	0.13	0.42	0.83	1.07	1.10	0.92	0.61	0.47	0.31				
Woods,1985,1987	Graphite (sputtered)	0.88	0.23	none	none	0.75	0.82	0.83	0.70	0.42	0.37	0.26				

Comparison of USU and Literature BSEY Values for Carbon

Table 7.3 Comparison of BSE yield measurements of graphitic carbon

Reference	Conditions	Parameters			BSE Yield at Incident Beam Energy (keV)										
		η_{max}	E_{max} (keV)	η at high E	0.1	0.2	0.3	0.5	1.0	1.5	2.0	2.5	3.0	5.0	10.0
MPG SEE Work	Graphite, (pyrolytic HOPG)	0.111	0.21	0.066	0.084	0.111	0.117	0.110	0.099					0.091	0.074
MPG SEE Work	Graphite, microcrystalline (Aquadag[TM])				0.291	0.230	0.173	0.165	0.158					0.100	0.080
MPG SEE Work	Graphitic amorphous carbon	0.192	0.32		0.140	0.182	0.196	0.181	0.148					0.126	
Bishop, 1963				0.06										0.085	0.072
Bronstein, 1969		0.15	0.4					0.149	0.15	0.133		0.107	0.088		
El Gomati, 1997				0.06						0.076	0.071	0.071	0.064	0.063	0.058	
Farhang, 1993	Disordered graphitic carbon (pocographite)		<0.1		0.32	0.26	0.23	0.20								
Heinrich, 1966				0.05												0.069
Hunger, 1979				0.05											0.082	0.066
Neubert, 1980				0.06												
Palluel, 1947		0.089	4.0	0.07								0.077		0.086	0.086	0.074
Philibert, 1963				0.06											0.08	0.06
Stemglass, 1953																
Stemglass, 1954		0.08	0.4				0.076		0.076	0.073	0.068	0.066				
Wintucky, 1981	Graphite (pyrolytic)								0.41	0.42	0.33	0.25				
Wintucky, 1981	Graphite, disordered (sputtered pyrolytic)								0.13	0.12	0.11	0.06				
Wintucky, 1981	Graphite, Turbostatic carbon (soot)								0.15	0.11	0.09	0.05				
Wittry,				0.05											0.082	

USU MPG Electron Emission Values for HOPG Carbon

Figure 7.6 is a plot of the residuals for the electron-induced electron emission spectra and the Chung and Everhart model, at incident energies of 500 eV and 85 eV for data shown in Figs. 7.4 and 7.5. The plots show there is a fine structure peak centered at 7.7 eV and 7.0 eV with 3.3 eV and 4.1 eV FWHM, respectively. This is attributed to the "σ peak" observed by Krieg [1982] that results from a maximum in the conduction band density of states due to σ-bands with weak dispersion near the Γ^{-}_{3A}-point [Painter, 1970]. Oellhafen and Frecouf [1983] have shown that this peak provides a fiduciary mark for very accurate calibration of the sample Fermi level. The energy position of the σ peak was found to be (7.57 ± 0.03) eV above the sample Fermi level [Oellhafen, 1983; Krieg, 1982], independent of emission angle, degree of graphite crystallinity, thermal annealing, incident electron energy, and excitation by electrons, UV photons, or x-ray photons. The sample and analyzer work functions, Φ_S and Φ_A, can be determined from the low energy cutoff of the electron emission spectrum, E_{sb}, by biasing the sample to the appropriate bias voltage, V_B. The cutoff is determined by, Φ_S if $-eV_B + \Phi_S > \Phi_A$ and by , Φ_A if $-eV_B + \Phi_S < \Phi_A$. Our measurements with V_B=0 V found E_{sb} equal to 0.04 eV and 1.2 eV, respectively, based on the Chung and Everhart model; this is in good agreement with values of 0.1 eV and 0.6 eV based on the difference between the theoretical and observed σ peak positions.

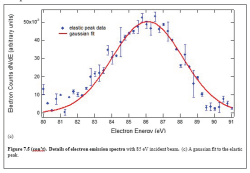


Figure 7.6 (cont'd). Details of electron emission spectra with 85 eV incident beam. (c) A gaussian fit to the elastic peak.

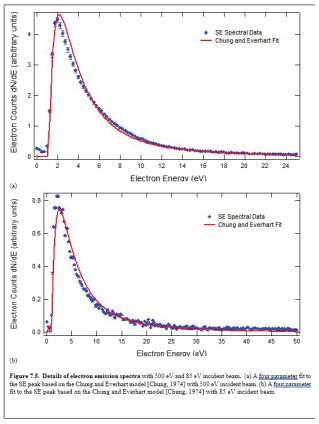


Figure 7.5. Details of electron emission spectra with 500 eV and 85 eV incident beam. (a) A four parameter fit to the SE peak based on the Chung and Everhart model [Chung, 1974] with 500 eV incident beam. (b) A four parameter fit to the SE peak based on the Chung and Everhart model [Chung, 1974] with 85 eV incident beam.

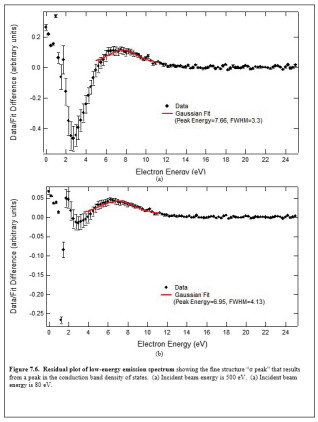
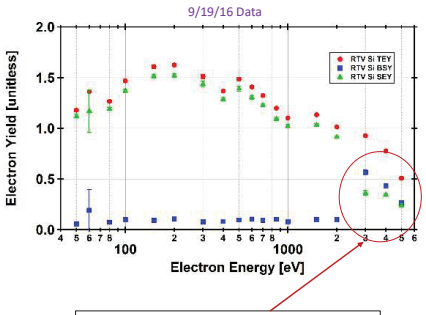
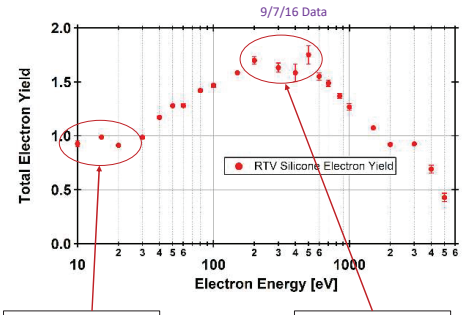


Figure 7.6. Residual plot of low-energy emission spectrum showing the fine structure "σ peak" that results from a peak in the conduction band density of states. (a) Incident beam energy is 500 eV. (a) Incident beam energy is 85 eV.

Effect of Insulator Charging on Yields--An Example for RTV Silicone Yield



Negative charging at high energies above E_2 causes yield to move towards unity. Note: low energy SE can gain enough energy to register as BSE, causing a drop in SEY and concomitant rise in BSEY..



Negative charging at low energies below E_1 causes TEY/SEY to move towards unity

Positive charging at intermediate energies near E_{max} causes TEY/SEY to be depressed. Note BSEY is not defined operationall below 50 eV.

TiN Alloy Total Electron Yield Curve Showing Charging Effects

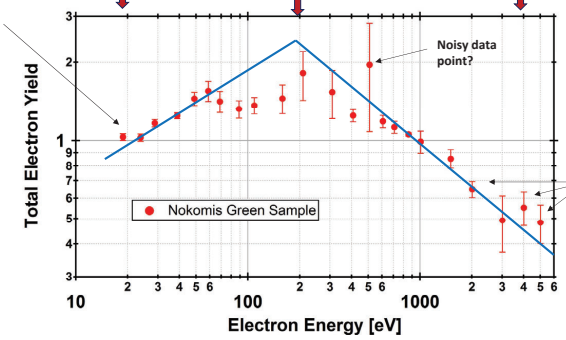
Charging Model

Negative charging effects below E1 at ~25 eV

Positive charging effects around E_{max}~220 eV from ~65 eV to ~550 eV

Negative charging effects below E1 at ~25 eV

Data may be noisy due to low yield or to negative charging. Yield values<30 eV may be higher than actual values due to stage bias.



Estimated uncharged "intrinsic" yield in blue

Question: Why would a conducting "green" layer show such large charging effects?

Data may be noisy due to low yield or to negative charging. BSE yield measurements should be able to distinguish these two options.

NASA/GRC

Secondary Electron Suppression with Carbonized Aerogels

Intermediate Report

References

References

- JR Dennison, Justin Christensen, Justin Dekany, Clint Thomson, Neal Nickles, Robert E. Davies, Mohamed Belhaj, Kazuhiro Toyoda, Arifur R. Khan, Kazutaka Kawasaki, Shunsuke Inoue, Isabel Montero, María E. Dávila and Leandro Olano, "Absolute Electron Emission Calibration: Round Robin Tests of Au and Polyimide," *Proceedings of the* 14*th Spacecraft Charging Technology Conference,* Space Research and Technology Centre of the European Space Agency (ESA/ESTEC), (Noordwijk, Netherlands, April 4-8, 2016) , 7 p.
- Gregory Wilson and JR Dennison, "*Approximation* of Range in Materials as a Function of Incident Electron Energy," *IEEE Trans. on Plasma Sci.*, **40**(2), 305-310 (2012). DOI: 10.1109/TPS.2011.2176515
- RC Hoffmann and JR Dennison, "Methods to Determine Total Electron-Induced Electron Yields Over Broad Range of Conductive and Nonconductive Materials," *IEEE Trans. on Plasma Sci.*, **40**(2), 298-304 (2012). DOI: 10.1109/TPS.2011.2178251
- Ryan Hoffmann, JR Dennison Clint D. Thomson and Jennifer Albretsen, "Low-fluence Electron Yields of Highly Insulating Materials" *IEEE Transaction on Plasma Science,* **36**(5) October 2008, 2238-2245. DOI: 10.1109/TPS.2008.2004226
- Peter Ramins, Henry G. Kosmahl, Dale Force, Raymond W. Palmer, James A. Dayton, Jr., "Verification of an improved computational design procedure for TWT-dynamic refocuser-MDC systems with secondary electron emission losses, IEEE Transactions on Electron Devices, vol. 33, p.85-90, Jan 1, 1986.
- Karl Vaden, and Isay L. Krainsky, "The Angular Distribution of Elastically Scattered Electrons and its Computed Effect on Collector Performance", Space Communication Technology Link, 2, No. 1, April 1999.
- I. L. Krainsky, "Computerized Device for Monitoring Secondary Electron Emission of Materials in the Pulse Mode", "The 2nd International Vacuum Electron Sources Conference" Tsukuba, Japan, July 7 – 10, 1998.

References

SE Yield

Bongler, R., Golla, U., Kussens, M., Reimer, L., Schendler, B., Senkel, R., Sprank, M. (1993), *Scanning* **15**, 1.

Bronstein, I M and Fraiman, B S, (1989), in *"Vtorichnava Elektronnava Emissiva"*, (Nanka, Moskva), p340.

Bruning, H., (1938), "Secondary electron emission," *Philips Tech. Rev.* **3**, 80-86.

Caron, M., Beuve, M., Rothard, H., Gervais, B., Dubus, A., Rosler, M., "Experimental and theoretical study of target thickness dependent *electron* yields induced by electrons in carbon," *Nucl. Instrum. Methods B* **135**, 436-442.

Farhang, H., Napchan, E., and Blott, B.H., "Electron backscattering and secondary electron emission from carbon targets comparison with Monte-Carlo simulations," *J. Appl. Phys*, **26**, 2266-2271 (1993).

Goto, K. and Takeichi, Y., "Carbon reference Auger electron spectra measured with a high-performance cylindrical mirror analyzer," *J. Vac. Sci. Technol. A* **14**, 1408-1415.

Kanava, K., Ono, S., (1984), in *"Electron Beam Interactions in Solids"*, ed. D. Kyser (SEM inc., Chicago), 69-98.

Kanava, K. and Kawakatsu, M. (1972) *J. Phys. D Appl. Phys.* **5**, 1727.

Moncrieff, D. A. Barker, P. R. (1976), *Scanning* **1**,195.

Reimer, L., Tolkamp, C., "Measuring the backscattering coefficient and secondary electron yield inside an SEM, (1990) *Scanning* **3**, 35.

Reimer, L., Drescher, H., "Secondary electron emission of 10-100 keV electrons from transparent films of Al and Au", *J. Phys. D Appl. Phys.*, **10**, 805-815, (1977).

Reimer, L., *Image Formation in Low-Voltage Scanning Electron Microscopy*, 144pp., SPIE, Bellingham, WA, (1995).

Rothwell, T. E., and Russell, P. E., in "Microbeam Analysis – 1988", ed. D, E, Newbury, (San Francisco Press, San Francisco, CA), 149.

Ruzic, D., Morre, R., Manos, D., and Cohen, S., (1982) "Secondary electron yields of carbon-coated and polished stainless steel," **20**, 1313-1316.

References

SE Yield

Sternglass, E. J., (1953), *"An experimental investigation of electron back-scattering and secondary emission from solids,"* Ph. D. thesis (Cornell University).

Whetten, N. R., (1965), 'Secondary electron emission of vacuum-cleaved solids," *J. Vac, Sci. Technol.*, **2**, 84-88.

Wintucky, E. G., Curran, A. N., Sovey, J. S., (1981), "Electron reflection and secondary emission characteristics of sputter-textured pyrolytic graphite surfaces," *Thin Solid Films* **84**, 161-169.

Wittry, D. B., (1966), *Proc. 4th Conf. on X-ray Optics and Microanalysis*, ed. R. Castaing et. Al. (Hermann, Paris), p. 168.

Woods, M. E., Hopkins, B. J., and McCraken, G. M., "Secondary electron yield measurements from limiter materials in the Joint European Torus," *Surf. Sci.*, **162**, 928-933 (1985).

Woods, M. E., Hopkins, B. J., Mattews, G. F., McCraken, G. M., Sewell, P. M., and Fahrang, H., "An investigation of the secondary electron emission of carbon samples exposed to a hydrogen plasma," *J. Appl. Phys.*, **20**, 1136-1142 (1987).

References

SE/BSE Spectra

Chang, M. S., and Everhart, T. E., "Simple calculation of energy distribution of low-energy secondary electrons emitted from metals under electron bombardment,:" *J. Appl. Phys.* **45**, 2, 707-709. (1974).

Goto, K. and Yoshinori, "Carbon reference Auger electron spectra measured with a high-performance cylindrical mirror analyzer," *J. Vac. Sci. Technol. A*, **14**, 1408-1414, (1996).

Hansen, W. N. and Hansen, G. J., "Standard reference surfaces for work function measurements in air," *Surf. Sci.*, **481**, 172-184.

Krieg, J., Gelhafen, P., and Guntherodt, H. J., "Observations of unfilled electron states in alkali intercalation compounds by secondary electron spectroscopy," *Solid State Comm.*, **42,** 831-833 (1982).

Oelhafen, P. and Freeouf, J. L., "Accurate spectrometer calibration in electron spectroscopy," *J. Vac, Sci. Technol. A*, **1**, 96-97.

Painter, G. S. and Ellis, D. E., "Electronic band structure and optical properties of graphite from a variational approach," *Phys. Rev. B*, **1**, 4747-4752 (1970).

References

BSE Yield

Bishop, H. E., (1963), Ph. D. Thesis, Cambridge.

Farhang, H., Napchan, E., and Blott, .B. H., "Electron backscattering and secondary electron emission from carbon targets: comparison of experimental results with Monte-Carlo simulations," *J. Appl. Phys.*, **26**, 2266-2271 *1993).

El Gomati, M. M. and Assad, A. M. D., *Proc. 5th European Workshop on Microbeam Analysis*, (in press).

Heinrich, K. F. J. (1996), *Proc. 4th Conf. on X-ray Optics and Microanalysis*, ed. R. Cataing, et. Al., (Hermann , Paris).

Hovington, P., Joy, D. C., Gauvin, R., and Evans, N., (1995), unpublished data. For a summary, see Joy D. C., Luo S., Gauvin R., Hovington P., and Evans, N. (1996), *Scanning Microscopy* **10**, 655-666.

Hungar H-J., Kuchler L., (1979), *Phys. Stat. Sol.,* (**a**) **56**, K45.

Kanter, H., "Zur Ruckstreuung von Elektronen im Energiebereich von 10 bis 100 keV," *Ann. Phys*, **6**, 20, 144-166, (1957).

Luo, S., Dunlap, J. R., and Joy, J. C., (1995), *Proc. 51st Ann. Meeting MSA*, ed. G. W. Bailey and C. L. Rieder, (San Francisco Press, San Francisco.)

Neubert, G., and Rogaschewski, S., "Backscattering coefficient measurements of 15-60 keV electrons for solids at various angles of incidence," *Phys. Stat. Sci. (a)*, **59**, 35-41, (1980).

Palluel, P., (1947), *Compt. Rendu.* **224**, 1492.

Philibert, J. and Weinryb, E. (1963), *Proc. 3rd Conf. on X-ray Optics and Microanalysis*, p.163, also *C. R. Acad. Sci.*, **256**, 4535 (1964).

Sternglass, E. J., 1953, "An experimental investigation of electron backscattering and secondary emission from solids," Ph. D. thesis (Cornell University).

Sternglass, E. J., "Backscattering of kilovolt electrons from solids," *Phys. Rev.*, **95**, 2, 345-358, (1954).

Wintucky, E. G., Curran, A. N., and Sovey, J. S., (1981), "Electron reflectance and secondary emission characteristics of sputter-textured pyrolytic graphite surfaces," *This Solid Films*, **84**, 161-169.